Developmental Cell
Short Article

RagA, but Not RagB, Is Essential for Embryonic Development and Adult Mice

Alejo Efeyan,[1,2,3,4,5] Lawrence D. Schweitzer,[1,2,3,4,5] Angelina M. Bilate,[1] Steven Chang,[1,2,3,4,5] Oktay Kirak,[1,6] Dudley W. Lamming,[1,2,3,4,5,7] and David M. Sabatini[1,2,3,4,5,*]
[1]Whitehead Institute for Biomedical Research, 9 Cambridge Center, Cambridge, MA 02142, USA
[2]Broad Institute of Harvard and MIT, 7 Cambridge Center, Cambridge, MA 02142, USA
[3]Department of Biology, Massachusetts Institute of Technology (MIT), Cambridge, MA 02139, USA
[4]David H. Koch Institute for Integrative Cancer Research at MIT, 77 Massachusetts Avenue, Cambridge, MA 02139, USA
[5]Howard Hughes Medical Institute, MIT, Cambridge, MA 02139, USA
[6]Present address: The Scripps Research Institute, 10550 North Torrey Pines Road, La Jolla, CA 92037, USA
[7]Present address: School of Medicine and Public Health, University of Wisconsin-Madison, Madison, WI 53705, USA
*Correspondence: sabatini@wi.mit.edu
http://dx.doi.org/10.1016/j.devcel.2014.03.017

SUMMARY

The mechanistic target of rapamycin complex 1 (mTORC1) integrates cues from growth factors and nutrients to control metabolism. In contrast to the growth factor input, genetic disruption of nutrient-dependent activation of mTORC1 in mammals remains unexplored. We engineered mice lacking RagA and RagB genes, which encode the GTPases responsible for mTORC1 activation by nutrients. RagB has limited expression, and its loss shows no effects on mammalian physiology. RagA deficiency leads to E10.5 embryonic death, loss of mTORC1 activity, and severe growth defects. Primary cells derived from these mice exhibit no regulation of mTORC1 by nutrients and maintain high sensitivity to growth factors. Deletion of RagA in adult mice is lethal. Upon RagA loss, a myeloid population expands in peripheral tissues. RagA-specific deletion in liver increases cellular responses to growth factors. These results show the essentiality of nutrient sensing for mTORC1 activity in mice and its suppression of PI3K/Akt signaling.

INTRODUCTION

The mechanistic target of rapamycin (mTOR) is a serine-threonine kinase that, as part of mTOR complex 1 (mTORC1), orchestrates cell growth and anabolism (Laplante and Sabatini, 2012). In mammals, mTORC1 activity is tightly controlled by growth factors, which trigger a cellular cascade that culminates in mTORC1 kinase activation. Nutrient abundance regulates mTORC1 through the activation of the Rag GTPases, which recruit mTORC1 to the lysosomal surface, an essential step for its kinase activation by growth factors. Hence, both inputs—growth factors and nutrients—must be present for maximal mTORC1 activity.

Germline deletion of the Raptor or mTOR genes in mice demonstrates the requirement for mTORC1 activity for mammalian development (Gangloff et al., 2004; Guertin et al., 2006; Murakami et al., 2004). In addition, acute deletion of Raptor in the tissues of adult mice showed that loss of mTORC1 activity in mammals has profound consequences (Polak and Hall, 2009). The physiological importance of growth factor-dependent regulation of mTORC1 in mammals is well established (Goorden et al., 2011). We have previously reported that constitutive RagA activity in mice leads to a neonatal energetic crisis and death (Efeyan et al., 2013), indicating that, unlike constitutive activation by growth factor signaling, constitutive activation of mTORC1 by the nutrient sensing pathway (i.e., amino acids and glucose) is compatible with embryonic development but has a detrimental role soon after birth. However, the requirement of the nutrient sensing machinery in mammals remains unexplored (reviewed in Efeyan and Sabatini, 2013; Laplante and Sabatini, 2012).

Here, we show that abrogation of nutrient-dependent activation of mTORC1, by means of genetic loss of the Rag GTPases, leads to embryonic lethality. Conditional deletion of RagA (but not RagB) in adult mice strongly suppresses mTORC1 activity and leads to PI3K/Akt activation. Furthermore, acute deletion of RagA in adult mice is also lethal and leads to the expansion of a monocytic-like population, which colonizes multiple organs.

RESULTS

RagA Is Essential for mTORC1 Activation and for Embryonic Development

We have previously generated mice conditionally expressing a constitutively active form of RagA ($RagA^{GTP}$), by means of a Lox-STOP-Lox strategy (Efeyan et al., 2013). In the absence of the Cre-recombinase, the $RagA^{STOP}$ allele is not expressed and is functionally null, and we took advantage of this prerecombined null allele to determine the consequences of the absence of the RagA gene in mice. While $RagA^{STOP/+}$ mice were viable and seemingly normal, $RagA^{STOP/STOP}$ mice succumbed embryonically. We also generated conventional RagA knockout mice by means of generating a RagA floxed ($RagA^{fl/fl}$) allele (Figure S1A available online). We then crossed $RagA^{fl/+}$ mice with CMV-Cre transgenic mice, which delete RagA in the germline (referred to as $RagA^{\Delta}$ or "deleted" allele). Through intercrosses of $RagA^{STOP/+}$ mice or $RagA^{\Delta/+}$ mice, we observed that deletion

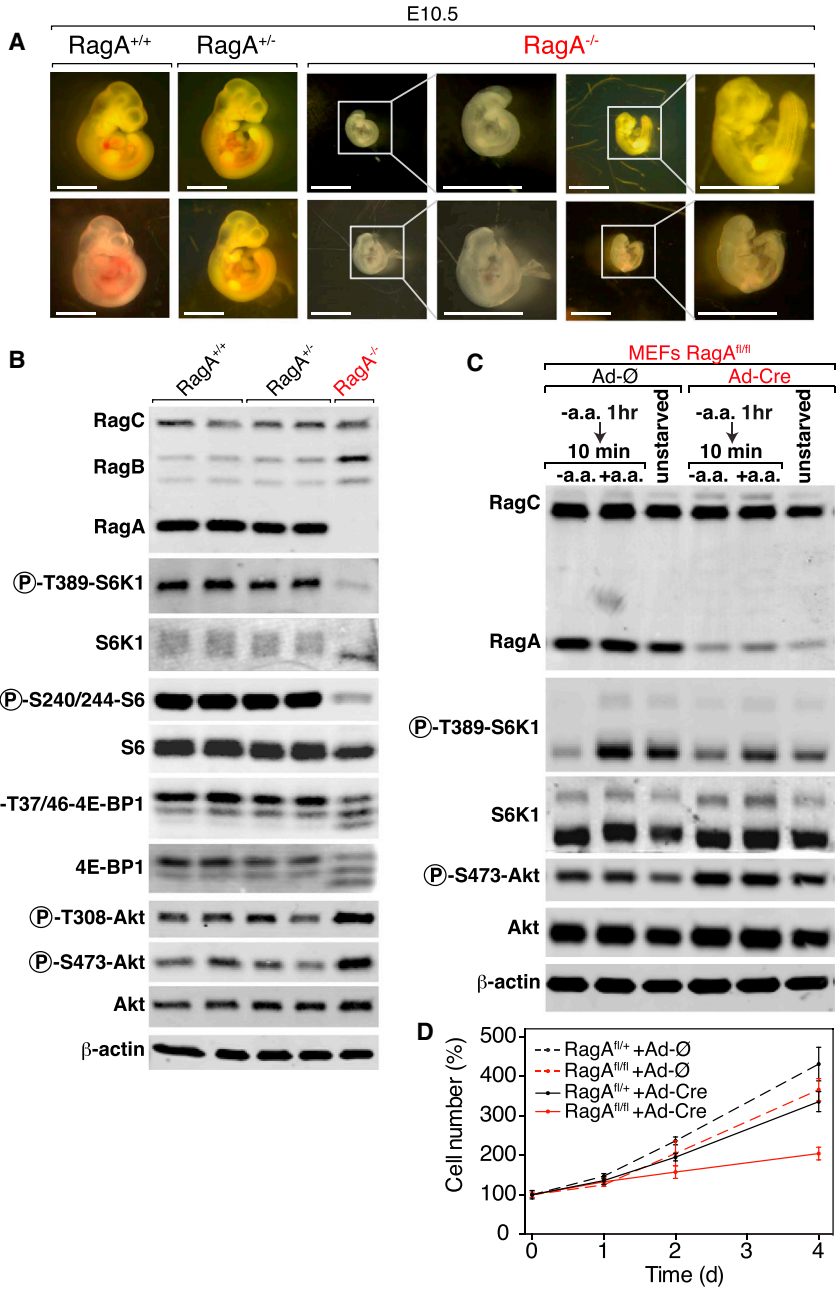

Figure 1. Embryonic Lethality of RagA KO Mice

(A) Representative pictures of E10.5 embryos of the indicated RagA genotype (see also Figure S1).

(B) Whole-embryo protein extracts from RagA$^{+/+}$, RagA$^{+/-}$, and RagA$^{-/-}$ littermates were analyzed by immunoblotting for the indicated proteins.

(C) RagA$^{fl/fl}$ MEFs were infected with control (Ad-Ø) or adenovirus encoding the Cre recombinase (Ad-Cre), starved for amino acids for 1 hr, and, where indicated, restimulated for 10 min. Total protein extracts were then analyzed by immunoblotting for the indicated proteins.

(D) Total cell count of cells infected as in (C) was monitored for 4 days. Data are mean ± SD; n = 3.

of RagA (RagA$^{-/-}$) led to embryonic lethality at ~E10.5 days (Table S1). Embryos lacking the RagA gene showed profound developmental aberrations, including an open neural tube and severely decreased size, and a proportion was evidently reabsorbed by 10 days (Figures 1A and S1B). Consistent with a key role for RagA in the activation of mTORC1 in vivo, mTORC1 activity was severely reduced in total protein extracts of embryos lacking the RagA gene (Figure 1B; additional examples in Figure S1C). It is unlikely that this reflects an overall decrease in cellular signaling secondary to reabsorption, as protein extracts were prepared from embryos with heartbeats, and furthermore, increased Akt activity, revealed by its phosphorylation at Thr308 or Ser473, was evident in RagA-deficient embryos (Figure 1B). Indeed, when two different RagA null E10.5 embryos were obtained in the same litter, one alive and one reabsorbed, the former showed high Akt activity, whereas the latter showed decreased Akt activity, when both were compared with wild-type (WT) embryos (Figure S1C). This result also shows the strong negative regulation that mTORC1 has on Akt activation, as shown previously (Harrington et al., 2004; Haruta et al., 2000; Um et al., 2004). RagB levels are very low or absent in most tissues of adult mice, and also in embryos. Interestingly, embryos lacking RagA frequently showed upregulation of RagB protein (Figures 1B and S1C), suggesting the existence of a mechanism that tries to maintain the total level of the Rag GTPases.

We established primary mouse embryonic fibroblasts (MEFs) cultures from RagA$^{fl/+}$ and RagA$^{fl/fl}$ E13.5 embryos and deleted the RagA gene by infecting the cells with adenovirus encoding Cre-recombinase. Acute loss of RagA led to partial loss of mTORC1 activation by amino acids or glucose, together with activation of Akt (Figures 1C, S1D, and S1E). This signaling defect was accompanied by a moderate decrease in proliferation rate (Figure 1D). As nondeleted, RagA$^{fl/fl}$ cells outcompeted RagA$^{\Delta/\Delta}$ cells, attempts to establish cell lines lacking RagA gene were not successful with this approach.

Nutrient-Insensitive mTORC1 Activity in RagA-Deficient Cells in Culture

To overcome out-competition of nonrecombining RagA$^{fl/fl}$ MEFs in the adenovirus-Cre-based approach, we attempted to obtain RagA$^{-/-}$ cells by culturing RagA E10.5 genetically deficient embryos. We readily obtained cultures from RagA-expressing embryos, but the proportion of RagA-deficient cell lines that survived initial in vitro conditions was very low. In addition, longer times in culture were necessary for RagA-deficient cells to start

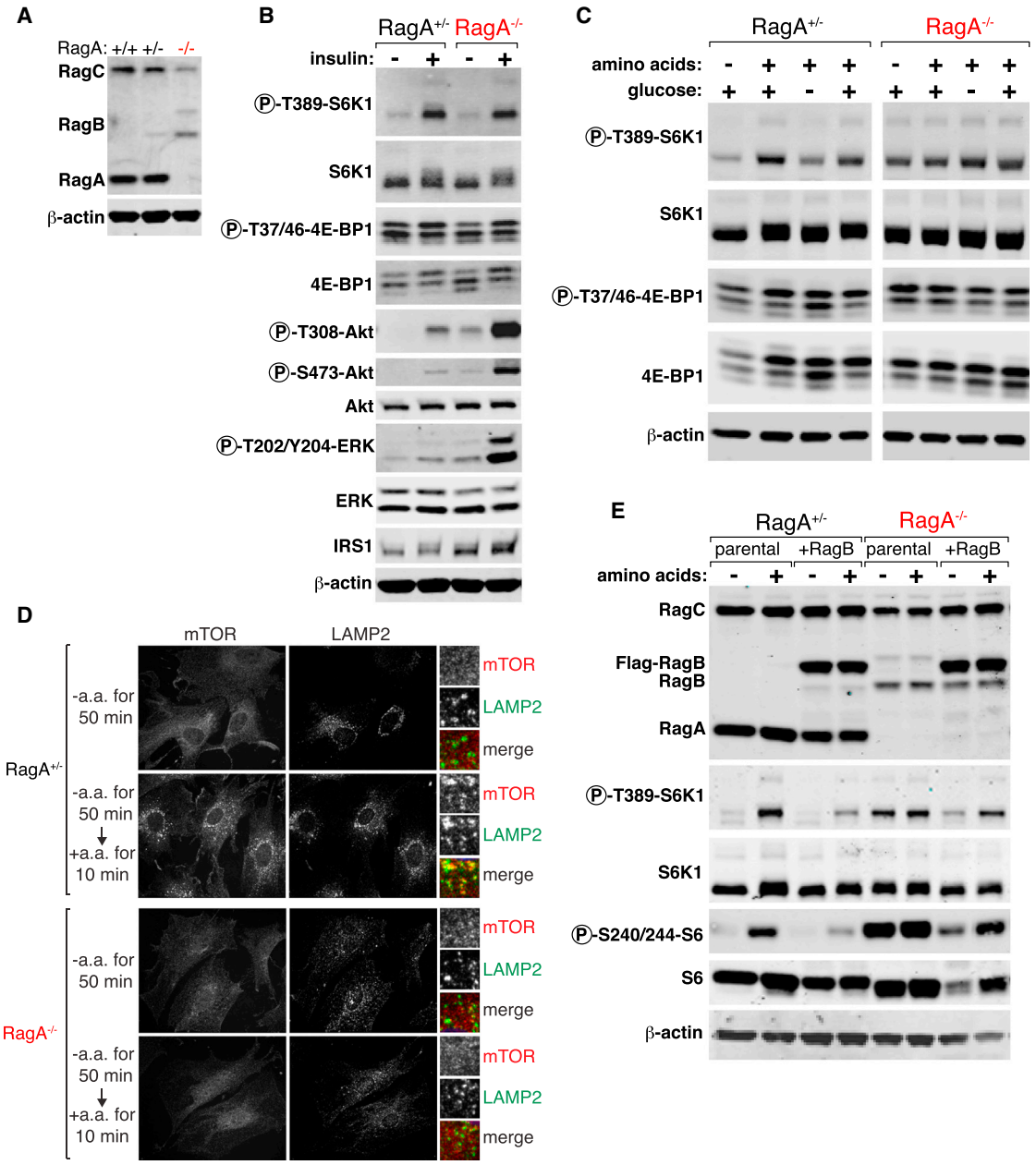

Figure 2. RagA Null Cells Exhibit Nutrient-Independent mTORC1 Activity

(A) Absence of RagA protein in surviving RagA$^{-/-}$ cell lines.

(B) RagA$^{-/-}$ cells maintain high sensitivity to growth factor deprivation, as determined by immunoblotting for mTORC1 and Akt activation markers.

(C) RagA$^{-/-}$ cells exhibit constitutive mTORC1 activity regardless of nutrient (amino acid or glucose) deprivation, as determined by immunoblotting for mTORC1 activation markers from whole-cell extract after amino acid or glucose starvation of cells followed by restimulation.

(D) mTOR localization by immunofluorescence. In RagA$^{+/-}$ cells, amino acid deprivation causes mTOR to localize to a diffuse puncta throughout the cytoplasm. Readdition of amino acids leads to mTOR shuttling to the lysosomal surface and colocalizing with the lysosomal protein Lamp2. In contrast, RagA$^{-/-}$ cells show mTOR constitutively diffuse throughout the cytoplasm, regardless of amino acid levels.

(E) Constitutive mTORC1 activity, regardless of amino acid levels, can be reversed by reconstituting Rag activity. RagA$^{-/-}$ cells were infected with a lentivirus encoding RagB^{WT} protein, and after starvation and restimulation with amino acids, whole-cell protein extracts were immunoblotted for the indicated proteins (see also Figure S2).

proliferating. Nevertheless, we managed to obtain several independent cell lines. As in the embryos, RagA-deficient cells showed a moderate upregulation of RagB (Figures 2A, S2A, and S2B). mTORC1 activity was inhibited by deprivation of amino acids, glucose, or growth factors (as determined by phosphorylation of S6K1 and 4EBP1) in RagA-proficient cells. In contrast, in RagA-deficient cells, mTORC1 activity was insensitive to deprivation of either amino acids or glucose but

maintained regulation by growth factors (Figures 2B and 2C). This suggests that loss of RagA led to the emergence of a RagA-independent mechanism of maintaining mTORC1 activity that contrasts with the very low mTORC1 activity of Ragulator-deficient cells (Sancak et al., 2010). It is unlikely that another kinase, in RagA-deficient cells, is responsible for phosphorylating S6K1 and 4EBP1, as inhibition of mTORC1 with rapamycin ablated the phosphorylation of S6K1 (Figure S2C). Furthermore, knockdown of the Rheb GTPase, responsible for stimulating the mTORC1 kinase activity and the endpoint of growth factor input, completely ablated mTORC1 activity in RagA$^{-/-}$ cells (Figure S2D). RagA-deficient cells also showed a marked increase in Akt activation, as determined by the phosphorylation of Thr308 and Ser473 on Akt, which likely helps to compensate for the decrease in mTORC1 caused by RagA loss (Figure 2B). In addition, increased levels of total IRS1 and a strong activation of the MAPK kinase pathway were also evident in these cells (Figure 2B), indicating that activation of growth factor signaling is not restricted to PI3K/Akt. We initially hypothesized that the increase in the abundance of RagB could rescue the loss of RagA in mTORC1 activation, allowing mTORC1 recruitment to the outer lysosomal surface, the site of mTORC1 activation. Inconsistent with this possibility, RagC, the obligate partner of RagA or RagB, did not colocalize with the lysosomal marker Lamp2 (Figure S2E), suggesting that a mild elevation in RagB levels could not overcome loss of RagA. Addition of amino acids in RagA-proficient cells recruited mTORC1 to the outer lysosomal surface (Sancak et al., 2008, 2010). In contrast, in cells lacking RagA, mTORC1 remained diffuse throughout the cytoplasm and did not colocalize with Lamp2 regardless of the presence or absence of amino acids (Figure 2D). To discard a qualitatively different lysosomal morphology that could mislead the interpretation of the results, we performed immunofluorescence staining for another lysosomal marker, Lamp1, in cells fixed in methanol. While methanol fixation precludes staining for mTORC1, it is optimal for preserving membrane structures and for the staining of membrane-bound proteins. We observed a similar lysosomal morphology in RagA-proficient and RagA-deficient cells stained for Lamp1 (Figure S2F). This suggested that a RagA-independent mechanism for maintaining mTORC1 activity was at work. In order to explore the reversibility of this phenomenon, we reconstituted Rag activity in RagA$^{-/-}$ cells by stably expressing RagB from a lentiviral plasmid. In these cells, mTORC1 activity was readily inhibited by amino acid withdrawal, and readdition of amino acids led to mTORC1 activation, thus correcting the insensitivity of RagA-deficient cells (Figure 2E). In agreement with this, forced expression of RagB allowed mTORC1 recruitment to the lysosome surface in the presence, but not in the absence, of amino acids (Figure S2G). In addition, expression of RagB in RagA$^{-/-}$ cells partially suppressed the activation of Akt (Figure S2H). The similar reversion of the nutrient-dependent regulation of mTORC1 activity was observed when we transduced RagA (Figure S2I), suggesting that overall Rag activity, rather than specific potential functions of RagA or RagB, was responsible for this rescue.

To analyze the consequences of the lack of regulation of mTORC1 activity by nutrients in RagA-deficient cells, we performed prolonged amino acid starvation and determined the extent to which autophagy, a cellular process of recycling cytoplasmic proteins and organelles that is regulated by mTORC1 (Mizushima et al., 2008), was affected in RagA-deficient cells. A 20 min amino acid starvation was sufficient to inhibit mTORC1 activity in RagA-proficient cells. However, prolonged amino acid starvation (i.e., at least 2 hr) was necessary for triggering inhibition of mTORC1 activity in RagA-deficient cells (Figure S2J). Interestingly, readdition of amino acids for 10 min resulted in no mTORC1 activation in RagA-deficient cells, showing that the mechanism leading to mTORC1 activation in the absence of RagA does not rely on a fast signal transduction cascade (Figure S2K). When we looked at the regulation of autophagy markers, we observed that phosphorylation of the mTORC1 target ULK1 was also affected with slower kinetics in RagA-deficient cells (Figure S2J). P62, which is degraded during the process of autophagy, decreased in RagA-proficient and RagA-deficient cells, suggesting that RagA null are able to trigger autophagy upon prolonged amino acid starvation. In agreement with this, all cells, regardless of RagA status, showed a similar rate of death upon long nutrient withdrawal from the culture medium (data not shown).

Deletion of the RagB Gene in Mice Is Innocuous

In order to determine the contribution of RagA versus RagB in the regulation of mTORC1 activity in mice, we generated RagB floxed mice by introducing LoxP sites flanking the endogenous exon 3 of RagB gene, encoded on the X chromosome (Figure S3A). RagB^{floxed} mice were crossed with CMV-Cre transgenic mice to achieve complete deletion of RagB in the germline. Intercrosses of RagB$^{+/-}$ mice produced RagB$^{+/+}$, RagB$^{+/-}$, and RagB$^{-/-}$ (or male RagB$^{-/0}$) offspring with normal Mendelian ratios, suggesting that loss of RagB has no obvious consequences for embryonic development or for surviving the first weeks of life. Deletion of the RagB gene was confirmed in RagB$^{-/0}$ mice in whole-brain extracts (Figure S3B). A redundant and hence compensatory role of RagA in the context of RagB null mice was very likely to occur, as RagA has a widespread pattern of expression in most tissues and is more abundant than RagB in tissues in which RagB is expressed to detectable levels, as in the brain (Figure S3B). Overall mTORC1 activity was not regulated in whole-mouse brain extracts upon fasting and refeeding, and more importantly, it was also not affected by loss of RagB (Figure S3C). In liver extracts, mTORC1 activity was equally regulated by fasting/refeeding in RagB$^{+/0}$ and RagB$^{-/0}$ mice. It is possible that RagB plays specialized roles in the brain or in other organs, but nevertheless, the undetectable effects of its deletion are in sharp contrast to the deep signaling impairment and embryonic death seen in RagA-deficient mice.

Germline Deletion of RagA and RagB

In order to ablate all RagA/B activity and determine if RagB was providing some level of compensation in the context of RagA loss, we generated RagA/B double knockout mice (RagA/B DKO). At E10.5, the developmental time point at which RagA knockout embryos were found with profound defects but were generally still alive, RagA/B DKO embryos were found in low proportions and undergoing reabsorption (Table S2). This suggests that in the absence of RagA, increased levels of RagB can sustain some mTORC1 activity in early stages of embryonic development, and also provides an explanation for

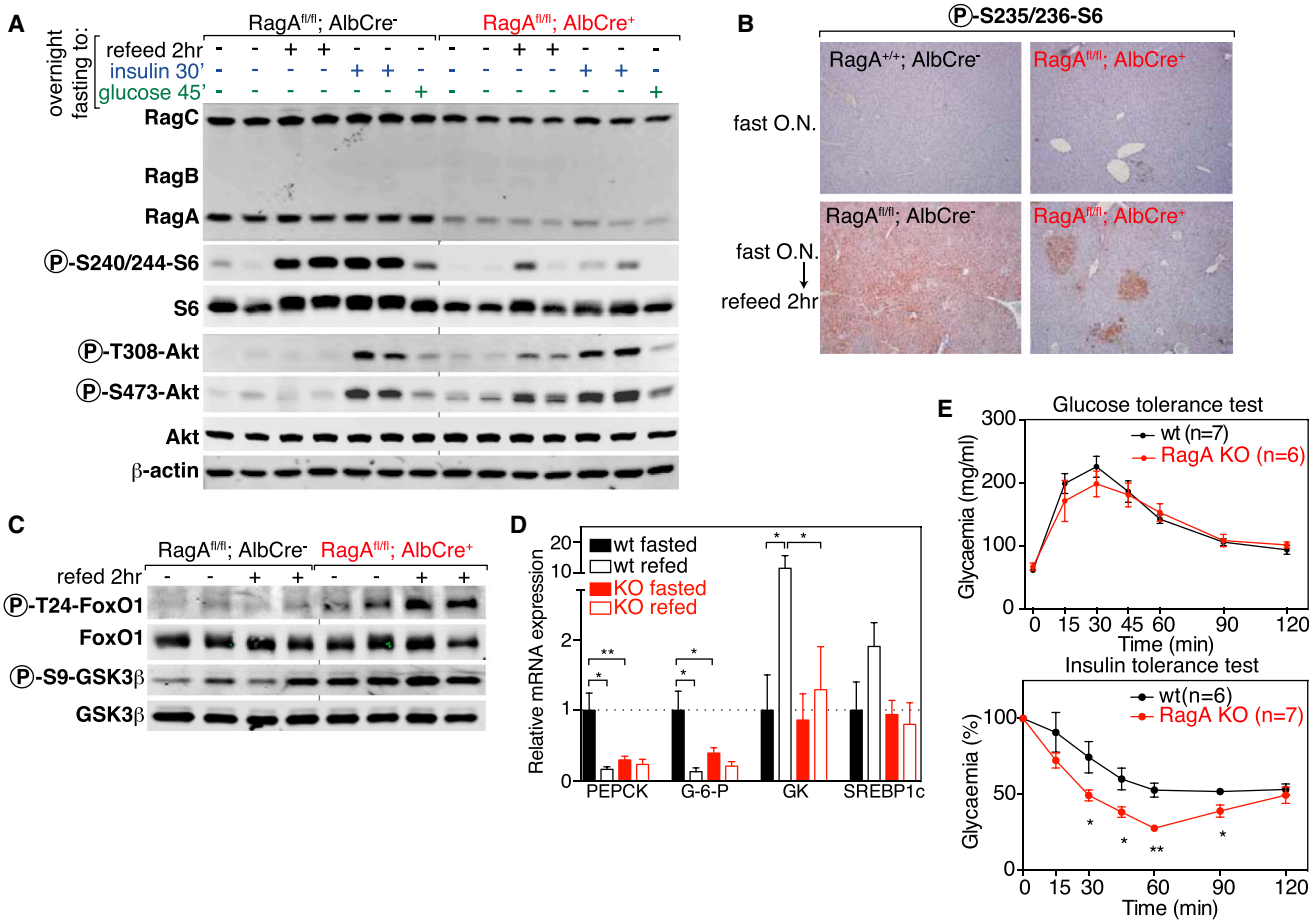

Figure 3. Defective mTORC1 Activation in RagA-Deficient Livers

(A) Mice of the indicated genotypes were starved overnight and then either refed or injected with glucose or insulin for the indicated times. Whole-protein extracts from liver were immunoblotted for indicated proteins.

(B) Samples as in (A) were analyzed by immunohistochemistry with anti-phospho-S235/236 S6 (see also Figure S3).

(C) Liver samples as in (A) were immunoblotted for Akt phosphorylation targets.

(D) RNA was extracted from control and RagA$^{fl/fl}$;Alb-Cre^{+} mice, and mRNA expression of the indicated genes was determined by quantitative real-time PCR (mean ± SEM, n = 5 (WT fasted), 3 (WT refed), 7 (KO fasted), 7 (KO refed).

(E) Glucose tolerance and insulin tolerance tests performed in WT and RagA liver KO mice (mean ± SEM). *p < 0.05; **p < 0.01.

the difference with the early death of mTOR null or Raptor null embryos (~E3.5 and ~E6.5, respectively; Gangloff et al., 2004; Guertin et al., 2006; Murakami et al., 2004). Ragulator null embryos, which ablate all Rag activity, but not other inputs to mTORC1, also succumbed before E10.5 (Teis et al., 2006), further suggesting a mild compensatory effect of RagB in RagA-deficient embryos.

Deletion of RagA and RagB in Hepatocytes

We analyzed the effect of acute loss of RagA in mouse liver, as it is a key organ for coordinating fasting/feeding responses and contributes greatly to glucose homeostasis. We deleted RagA and RagB genes in mouse livers in which Cre recombinase was under the expression of the albumin promoter (Alb-Cre) (Postic et al., 1999). Deletion of RagA in liver led to robust suppression of mTORC1 activity upon overnight fasting and refeeding, as seen by abrogated phosphorylation of mTORC1 targets in immunoblots (Figures 3A and S3D). Profound effects on mTORC1 activation were also observed when glucose or insulin were injected, showing the essentiality of RagA upstream of mTORC1 to allow its activation by the other main activator of mTORC1, growth factors. Similar results were observed when we assessed the phosphorylation of S6 by immunohistochemistry (Figure 3B). Isolated groups of cells in RagA$^{fl/fl}$;Alb-Cre^{+} mice showed an increase in phospho-S6 upon refeeding, which were clearly identified as hepatocytes at higher magnification (Figure S3E) and may be escapers from Cre-mediated recombination. This explains, together with nonhepatocyte cells present in the liver, the residual levels of RagA in western blots. When the same fasting/refeeding experiment was performed in old (>1 year) mice, regulation of mTORC1 activity was similar to that of wild-type mice (Figure S3F), and to a large extent, so were levels of the RagA protein, suggesting the possibility that a proportion of cells that had escaped Cre-mediated DNA recombination increased with time.

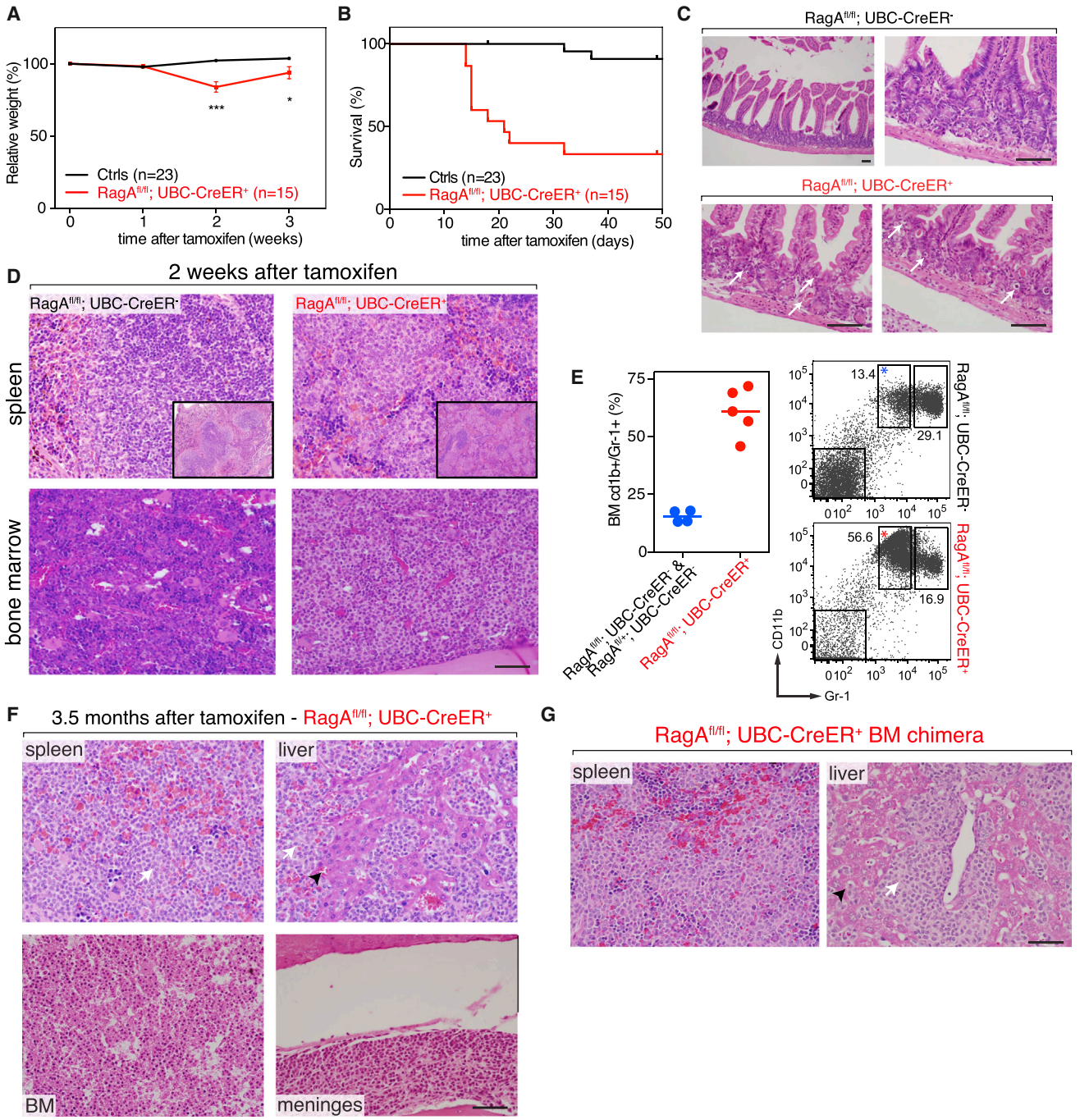

Figure 4. Acute Deletion of RagA in Adult Mice

(A) Control (RagA$^{fl/+}$;UBC-CreER^{-}, RagA$^{fl/+}$;UBC-CreER^{+}, RagA$^{fl/fl}$;UBC-CreER^{-}) and RagA$^{fl/fl}$;UBC-CreER^{+} mice were injected with tamoxifen for Cre activation, and their weight was monitored every week (mean ± SEM).

(B) Kaplan-Meier survival curves after tamoxifen injection of control (RagA$^{fl/+}$;UBC-CreER^{-}, RagA$^{fl/+}$;UBC-CreER^{+}, RagA$^{fl/fl}$;UBC-CreER^{-}) versus RagA$^{fl/fl}$;UBC-CreER^{+} mice.

(C) Representative hematoxylin and eosin (H&E)-stained sections of small intestine from RagA$^{fl/fl}$;UBC-CreER^{-} mice and RagA$^{fl/fl}$;UBC-CreER^{+} mice 2 weeks after start of tamoxifen injections. Arrowhead indicates apoptotic figures.

(D) Representative H&E-stained sections spleen and bone marrow from RagA$^{fl/fl}$;UBC-CreER^{-} mice and RagA$^{fl/fl}$;UBC-CreER^{+} mice 2 weeks after start of tamoxifen.

(E) Bone marrow cells were harvested, immunostained, and analyzed by flow cytometry. Dot plots show the cells gated on Lin^{-} (CD3/CD19/Ter119/NK1.1) and are representative of one mouse out of 4–5. Gr-1 and CD11b staining was used to identify monocytes. Graph shows the quantification of the proportion of resident (or patrolling) BM monocytes (determined by CD11b^{+} Gr-1^{low}). CD11b^{+} Gr-1^{high} corresponds to inflammatory monocytes.

(legend continued on next page)

Because RagA$^{-/-}$ livers showed a mild increase in RagB protein (Figures 3A and S3D), and in order to determine the impact of complete loss of Rag function, we generated RagA$^{fl/fl}$;RagB$^{fl/fl\ (or\ fl/0)}$;AlbCre^{+} mice (RagA/B DKO). In comparison to RagA KO livers, RagA/B DKO livers showed a further decrease in mTORC1 activity, again with hyperactivation of Akt (Figure S3G). This suggests that, as in embryos, RagB partially compensates for RagA loss in the activation of mTORC1.

We searched for the consequences of reduced mTORC1 activity and increased PI3K/Akt activities in RagA$^{-/-}$ livers on fasting/refeeding responses. FoxO1/3 and GSK3β, downstream phosphorylation targets of Akt involved in the regulation of glucose homeostasis, showed increased phosphorylation from fasted/refed RagA$^{-/-}$ livers (Figure 3C). As expected from the increased inhibitory phosphorylation of the FoxO transcription factors, we observed transcriptional changes in genes regulated by fasting/refeeding via the PI3K/Akt/FoxO axis, such as PEPCK, glucose-6-phosphatase, and glucokinase (Zhang et al., 2006) (Figure 3D). This correlated with a mild reduction in ad libitum blood glucose levels (Figure S3H) in young RagA$^{fl/fl}$;AlbCre^{+} mice. While the mice were equally tolerant to glucose in a glucose tolerance test (GTT), an increased reduction in glycaemia upon injection of insulin in an insulin tolerance test (ITT) was observed (Figure 3E), suggesting that loss of RagA leads to a better response to insulin in vivo. Together with the cell-autonomous effects on Akt activation in cultured RagA null cells, these findings provide support for the efficiency of dieting (i.e., reduced nutrient intake) and pure mTORC1 inhibitors to control overactivation of mTORC1, and for ameliorate insulin resistance and metabolic syndrome.

Deletion of RagA in Adult Mice Is Lethal

Because deletion of RagA in the germline led to embryonic lethality, precluding the analysis of adult RagA-deficient mice, we took advantage of a tamoxifen-inducible Cre-recombinase driven by a ubiquitous promoter (UBC-CRE-ERT2, also denoted herein as UBC-CreER) (Ruzankina et al., 2007), to achieve full-body acute deletion of RagA in adult mice. Injecting mice with tamoxifen caused excision of RagA and decreased mTORC1 activity in several tissues (Figures S4A and S4B). RagA$^{fl/fl}$;UBC-CreER^{+} (RagA-iKO) mice transiently lost ∼20% body weight within 1 week (Figure 4A). More than 50% of RagA-iKO mice succumbed within 2–3 weeks after the start of tamoxifen injections (Figure 4B). The time of death suggested atrophy of the small intestine, which has also been reported for full-body Raptor$^{\Delta/\Delta}$ mice (Hoshii et al., 2012). Indeed, the small intestine in RagA-iKO mice showed frequent apoptotic figures (Figure 4C).

In addition, RagA-iKO showed a prominent accumulation of cells that resembled monocytes in spleen and bone marrow (Figure 4D). Immunostaining using antibodies against monocyte surface markers confirmed the increase proportion of monocytes in bone marrow and spleen of RagA-iKO compared to their wild-type counterparts (Figure 4E). We then assessed the proliferative status of this lineage by in vivo bromodeoxiuridine (BrdU) incorporation. A population of CD11b^{low} Gr-1^{+} CD115^{-} cells from bone marrow of RagA-iKO incorporated nearly twice as much BrdU as did control mice (Figure S4C). The rapid expansion of monocytes was accompanied by a profound reduction in B lymphocytes and/or their progenitors (Figure S4D), as shown previously for Raptor-deleted mice (Hoshii et al., 2012; Kalaitzidis et al., 2012).

The rapid death (within 2–3 weeks) of RagA-iKO mice presumably due to intestinal atrophy was partially penetrant. In the ∼40% of mice that survived acute deletion of the RagA gene, the expansion of myeloid cells that could be already detected 2 weeks after tamoxifen, continued to spread in peripheral tissues. It was evident in liver, spleen, and meninges (Figure 4F) and in many cases was so severe that mice had to be sacrificed. This disease was histopathologically reminiscent of histiocytic sarcoma, the murine equivalent of monocytic leukemia, and did not stem from escapers from the action of the Cre recombinase, as the deletion of the RagA gene was confirmed by PCR (Figure S4E). Furthermore, spleen and purified splenocytes, as well as liver from treated RagA-iKO mice, showed barely detectable levels of RagA protein and low mTORC1 activity (Figure S4F). In addition, cultured macrophages obtained from RagA-iKO mice 2 weeks after starting tamoxifen treatment showed reduced levels of RagA, reduced mTORC1 activation, and increased Akt activity (Figure S4G).

We also performed bone marrow reconstitution experiments to analyze this myeloid expansion without the detrimental effects of RagA deletion in other tissues, such as the small intestine. Irradiated wild-type hosts were reconstituted with bone marrow cells from either RagA$^{fl/fl}$;UBC-CreER^{+} or RagA$^{fl/fl}$;UBC-CreER^{-} mice and treated with tamoxifen after engraftment. Tamoxifen injections in bone marrow chimeras did not lead to the acute (within 2–3 weeks) death observed in full-body RagA$^{fl/fl}$;UBC-CreER^{+} mice. However, RagA$^{fl/fl}$;UBC-CreER^{+} chimeras recapitulated the splenomegaly (Figure S4H) and the monocyte expansion in bone marrow and peripheral tissues (Figure 4G) that was observed in full-body RagA-iKO mice and that limited their survival.

DISCUSSION

Absence of RagB in embryos and mice did not show any consequences, had no obvious phenotypes, and were fertile. This is consistent with the limited expression of the RagB gene in most tissues and with the higher expression of RagA throughout the body. In contrast, RagA null embryos succumbed within ∼10–11 days of development, with profound defects and a severe reduction in mTORC1 activity. On the one hand, RagA-deficient embryos demonstrate the requirement of the nutrient dependent input upstream of mTORC1 for its activity. The similar onset of lethality with Rheb-deficient embryos (Goorden et al., 2011) indicates that both major regulators of

(F) Representative H&E-stained sections of indicated tissues from RagA$^{fl/fl}$;UBC-CreER^{-} mice and RagA$^{fl/fl}$;UBC-CreER^{+} mice 3.5 months after tamoxifen injections. Black arrowhead indicates normal tissue; white arrowhead indicates monocytic population.

(G) Representative H&E-stained sections of liver and spleen from wild-type mice reconstituted with bone marrow from RagA$^{fl/fl}$;UBC-CreER^{-} mice and RagA$^{fl/fl}$;UBC-CreER^{+} mice, injected with tamoxifen 6 weeks after bone marrow reconstitution (see also Figure S4). Black arrowhead indicates normal tissue; white arrowhead indicates monocytic population. Bar indicates 40 μm.

mTORC1 are essential for life. On the other hand, the difference in the onset of death between RagA null and mTOR null (or Raptor null) embryos can be explained by residual mTORC1 activity in the absence of RagA, which may be due to increased levels of RagB. Finally, the relatively high levels of RagA in all tissues can explain the lack of phenotypes associated with RagB deletion.

The inability to acutely induce deletion of RagA in MEFs prompted us to establish cell lines from E10.5 embryos genetically deficient for RagA. To our surprise, instead of having residual mTORC1 activity, these lines grew with comparable levels of mTORC1 activity that did not respond to acute changes in nutrients, but were able to regulate mTORC1 via slow, perhaps transcriptionally regulated mechanisms. Interestingly, it was recently shown that Rheb null cells also retain significant levels of mTORC1 activity in culture (Groenewoud et al., 2013). In RagA null cells, mTORC1 did not localize at the lysosomal surface, indicating that cells underwent an adaptation that enabled high mTORC1 activity in a Rag-independent manner and that involved an upregulation of the growth factor input.

The effects of the liver-specific ablation of Rag function on mTORC1 activity were severe and comparable to Raptor loss (Sengupta et al., 2010). Deletion of RagA led to activation of PI3K/Akt and downstream inhibition of the FoxO1/3 transcription factors. Because the FoxO transcriptional program increases de novo glucose production, glycaemia in ad libitum hepatocyte-specific RagA null mice was mildly lower. This result has implications in the context of metabolic syndrome therapeutic approaches, as nutrient overload has a strong correlation with the onset of type 2 diabetes (Wang et al., 2011). The data suggest that Rag-dependent regulation of mTORC1 may play a significant role in the correction of insulin resistance and glucose homeostasis observed when nutrient intake is lowered. Interestingly, the biguanide metformin, used to control glucose output in the liver, has been reported to inhibit, among other pathways, the Rag GTPases (Kalender et al., 2010). The data presented herein are consistent with at least part of the beneficial effects of metformin being related to its effects on the regulation of Rag-dependent mTORC1 activation.

Our work shows that deletion of the RagA gene in adult mice leads to many changes similar to those resulting from the loss of the key mTORC1 component Raptor. This is highlighted by the rapid death following tamoxifen injection in adult $RagA^{fl/fl}$; UBC-$CreER^{+}$ mice. Deletion of RagA leads to a rapid expansion of a similar population that is found in meninges, liver, and other tissues and limits survival. PTEN deletion, which leads to Akt activation, can also lead to different types of myeloproliferative disease (Tesio et al., 2013; Yilmaz et al., 2006), again linking reduced mTORC1 activity with increased PI3K/Akt activity.

The solid body of evidence pointing toward mTORC1 as a key regulator of aging is supported by the antiaging and antitumoral effects of rapamycin, a specific, albeit incomplete, mTORC1 inhibitor. The realization that rapamycin can also block mTORC2 (Lamming et al., 2012; Sarbassov et al., 2006), as mTOR-catalytic inhibitors do (Laplante and Sabatini, 2012), has spurred interest in the development of pure (and complete) mTORC1 inhibitors, that spare mTORC2 as an antiaging strategy. The results presented herein provide support for beneficial effects of such compounds on insulin sensitivity.

EXPERIMENTAL PROCEDURES

Generation of RagA and RagB Knockout Mice

All animal studies and procedures were approved by the MIT Institutional Animal Care and Use Committee. RagA locus was targeted by introducing LoxP sites and frt-neomycin-frt cassette flanking RagA exon (a map of the targeting allele is shown in Figure S1A). Similarly, the RagB locus was targeted by introducing LoxP sites flanking exon 3 (a map of the RagB targeting allele is shown in Figure S3A). $RagA^{STOP}$ allele was previously described (Efeyan et al., 2013).

Treatments of Mice

Fasting was performed from 6 p.m. to 9 a.m., and then mice were injected with 30% w/v glucose in PBS 100 μl per 30 g mouse, allowed to feed ad libitum, or injected intraperitoneally with 11.25 μl of insulin (HumulinR, Lilly) dissolved in 5 ml of PBS at a dose of 100 μl per 30 g mouse.

Treatments of MEFs

Subconfluent cells were rinsed twice and incubated in RPMI without amino acids and/or glucose and supplemented with 10% dialyzed fetal bovine serum, as described previously (Sancak et al., 2008). Stimulation with glucose (5 mM) or amino acids (concentration as in RPMI) was performed for 10 min. For serum withdrawal, cells were rinsed twice in serum-free Dulbecco's modified Eagle's medium (DMEM) and incubated in serum-free DMEM for the indicated times; 100 nM was used for insulin stimulation.

Statistical Analyses

For Kaplan-Meier survival curves, comparisons were made with the log-rank Mantel-Cox method. For quantitative real-time PCR analyses, measurements of glycemia, and other comparisons between pairs, nonparametric t tests were performed.

See Supplemental Experimental Procedures for details.

SUPPLEMENTAL INFORMATION

Supplemental Information includes four figures, two tables, and Supplemental Experimental Procedures and can be found with this article online at http://dx.doi.org/10.1016/j.devcel.2014.03.017.

ACKNOWLEDGMENTS

We thank members of the Sabatini Lab for helpful suggestions and Amanda Hutchins and Samantha Murphy for technical assistance. This work was supported by grants from the NIH (R01 CA129105, CA103866, and AI047389; R21 AG042876) and awards from the American Federation for Aging, Starr Foundation, Koch Institute Frontier Research Program, and the Ellison Medical Foundation to D.M.S., and by fellowships from the Human Frontiers Science Program and Charles King's Trust Foundation/Fortin Fellowship to A.E. L.D.S is a recipient of NCI Fellowship F31CA167872. D.W.L. is supported by an NIH K99/R00 Pathway to Independence Award (AG041765). D.M.S. is an investigator of Howard Hughes Medical Institute.

Received: November 1, 2013
Revised: March 10, 2014
Accepted: March 23, 2014
Published: April 24, 2014

REFERENCES

Efeyan, A., and Sabatini, D.M. (2013). Nutrients and growth factors in mTORC1 activation. Biochem. Soc. Trans. *41*, 902–905.

Efeyan, A., Zoncu, R., Chang, S., Gumper, I., Snitkin, H., Wolfson, R.L., Kirak, O., Sabatini, D.D., and Sabatini, D.M. (2013). Regulation of mTORC1 by the Rag GTPases is necessary for neonatal autophagy and survival. Nature *493*, 679–683.

Gangloff, Y.G., Mueller, M., Dann, S.G., Svoboda, P., Sticker, M., Spetz, J.F., Um, S.H., Brown, E.J., Cereghini, S., Thomas, G., and Kozma, S.C. (2004).

Disruption of the mouse mTOR gene leads to early postimplantation lethality and prohibits embryonic stem cell development. Mol. Cell. Biol. *24*, 9508–9516.

Goorden, S.M., Hoogeveen-Westerveld, M., Cheng, C., van Woerden, G.M., Mozaffari, M., Post, L., Duckers, H.J., Nellist, M., and Elgersma, Y. (2011). Rheb is essential for murine development. Mol. Cell. Biol. *31*, 1672–1678.

Groenewoud, M.J., Goorden, S.M., Kassies, J., Pellis-van Berkel, W., Lamb, R.F., Elgersma, Y., and Zwartkruis, F.J. (2013). Mammalian target of rapamycin complex I (mTORC1) activity in ras homologue enriched in brain (Rheb)-deficient mouse embryonic fibroblasts. PLoS ONE *8*, e81649.

Guertin, D.A., Stevens, D.M., Thoreen, C.C., Burds, A.A., Kalaany, N.Y., Moffat, J., Brown, M., Fitzgerald, K.J., and Sabatini, D.M. (2006). Ablation in mice of the mTORC components raptor, rictor, or mLST8 reveals that mTORC2 is required for signaling to Akt-FOXO and PKCalpha, but not S6K1. Dev. Cell *11*, 859–871.

Harrington, L.S., Findlay, G.M., Gray, A., Tolkacheva, T., Wigfield, S., Rebholz, H., Barnett, J., Leslie, N.R., Cheng, S., Shepherd, P.R., et al. (2004). The TSC1-2 tumor suppressor controls insulin-PI3K signaling via regulation of IRS proteins. J. Cell Biol. *166*, 213–223.

Haruta, T., Uno, T., Kawahara, J., Takano, A., Egawa, K., Sharma, P.M., Olefsky, J.M., and Kobayashi, M. (2000). A rapamycin-sensitive pathway down-regulates insulin signaling via phosphorylation and proteasomal degradation of insulin receptor substrate-1. Mol. Endocrinol. *14*, 783–794.

Hoshii, T., Tadokoro, Y., Naka, K., Ooshio, T., Muraguchi, T., Sugiyama, N., Soga, T., Araki, K., Yamamura, K., and Hirao, A. (2012). mTORC1 is essential for leukemia propagation but not stem cell self-renewal. J. Clin. Invest. *122*, 2114–2129.

Kalaitzidis, D., Sykes, S.M., Wang, Z., Punt, N., Tang, Y., Ragu, C., Sinha, A.U., Lane, S.W., Souza, A.L., Clish, C.B., et al. (2012). mTOR complex 1 plays critical roles in hematopoiesis and Pten-loss-evoked leukemogenesis. Cell Stem Cell *11*, 429–439.

Kalender, A., Selvaraj, A., Kim, S.Y., Gulati, P., Brûlé, S., Viollet, B., Kemp, B.E., Bardeesy, N., Dennis, P., Schlager, J.J., et al. (2010). Metformin, independent of AMPK, inhibits mTORC1 in a rag GTPase-dependent manner. Cell Metab. *11*, 390–401.

Lamming, D.W., Ye, L., Katajisto, P., Goncalves, M.D., Saitoh, M., Stevens, D.M., Davis, J.G., Salmon, A.B., Richardson, A., Ahima, R.S., et al. (2012). Rapamycin-induced insulin resistance is mediated by mTORC2 loss and uncoupled from longevity. Science *335*, 1638–1643.

Laplante, M., and Sabatini, D.M. (2012). mTOR signaling in growth control and disease. Cell *149*, 274–293.

Mizushima, N., Levine, B., Cuervo, A.M., and Klionsky, D.J. (2008). Autophagy fights disease through cellular self-digestion. Nature *451*, 1069–1075.

Murakami, M., Ichisaka, T., Maeda, M., Oshiro, N., Hara, K., Edenhofer, F., Kiyama, H., Yonezawa, K., and Yamanaka, S. (2004). mTOR is essential for growth and proliferation in early mouse embryos and embryonic stem cells. Mol. Cell. Biol. *24*, 6710–6718.

Polak, P., and Hall, M.N. (2009). mTOR and the control of whole body metabolism. Curr. Opin. Cell Biol. *21*, 209–218.

Postic, C., Shiota, M., Niswender, K.D., Jetton, T.L., Chen, Y., Moates, J.M., Shelton, K.D., Lindner, J., Cherrington, A.D., and Magnuson, M.A. (1999). Dual roles for glucokinase in glucose homeostasis as determined by liver and pancreatic beta cell-specific gene knock-outs using Cre recombinase. J. Biol. Chem. *274*, 305–315.

Ruzankina, Y., Pinzon-Guzman, C., Asare, A., Ong, T., Pontano, L., Cotsarelis, G., Zediak, V.P., Velez, M., Bhandoola, A., and Brown, E.J. (2007). Deletion of the developmentally essential gene ATR in adult mice leads to age-related phenotypes and stem cell loss. Cell Stem Cell *1*, 113–126.

Sancak, Y., Peterson, T.R., Shaul, Y.D., Lindquist, R.A., Thoreen, C.C., Bar-Peled, L., and Sabatini, D.M. (2008). The Rag GTPases bind raptor and mediate amino acid signaling to mTORC1. Science *320*, 1496–1501.

Sancak, Y., Bar-Peled, L., Zoncu, R., Markhard, A.L., Nada, S., and Sabatini, D.M. (2010). Ragulator-Rag complex targets mTORC1 to the lysosomal surface and is necessary for its activation by amino acids. Cell *141*, 290–303.

Sarbassov, D.D., Ali, S.M., Sengupta, S., Sheen, J.H., Hsu, P.P., Bagley, A.F., Markhard, A.L., and Sabatini, D.M. (2006). Prolonged rapamycin treatment inhibits mTORC2 assembly and Akt/PKB. Mol. Cell *22*, 159–168.

Sengupta, S., Peterson, T.R., Laplante, M., Oh, S., and Sabatini, D.M. (2010). mTORC1 controls fasting-induced ketogenesis and its modulation by ageing. Nature *468*, 1100–1104.

Teis, D., Taub, N., Kurzbauer, R., Hilber, D., de Araujo, M.E., Erlacher, M., Offterdinger, M., Villunger, A., Geley, S., Bohn, G., et al. (2006). p14-MP1-MEK1 signaling regulates endosomal traffic and cellular proliferation during tissue homeostasis. J. Cell Biol. *175*, 861–868.

Tesio, M., Oser, G.M., Baccelli, I., Blanco-Bose, W., Wu, H., Göthert, J.R., Kogan, S.C., and Trumpp, A. (2013). Pten loss in the bone marrow leads to G-CSF-mediated HSC mobilization. J. Exp. Med. *210*, 2337–2349.

Um, S.H., Frigerio, F., Watanabe, M., Picard, F., Joaquin, M., Sticker, M., Fumagalli, S., Allegrini, P.R., Kozma, S.C., Auwerx, J., and Thomas, G. (2004). Absence of S6K1 protects against age- and diet-induced obesity while enhancing insulin sensitivity. Nature *431*, 200–205.

Wang, T.J., Larson, M.G., Vasan, R.S., Cheng, S., Rhee, E.P., McCabe, E., Lewis, G.D., Fox, C.S., Jacques, P.F., Fernandez, C., et al. (2011). Metabolite profiles and the risk of developing diabetes. Nat. Med. *17*, 448–453.

Yilmaz, O.H., Valdez, R., Theisen, B.K., Guo, W., Ferguson, D.O., Wu, H., and Morrison, S.J. (2006). Pten dependence distinguishes haematopoietic stem cells from leukaemia-initiating cells. Nature *441*, 475–482.

Zhang, W., Patil, S., Chauhan, B., Guo, S., Powell, D.R., Le, J., Klotsas, A., Matika, R., Xiao, X., Franks, R., et al. (2006). FoxO1 regulates multiple metabolic pathways in the liver: effects on gluconeogenic, glycolytic, and lipogenic gene expression. J. Biol. Chem. *281*, 10105–10117.

Developmental Cell, Volume *29*

Supplemental Information

RagA, but Not RagB, Is Essential for Embryonic Development and Adult Mice

Alejo Efeyan, Lawrence D. Schweitzer, Angelina M. Bilate, Steven Chang, Oktay Kirak, Dudley W. Lamming, and David M. Sabatini

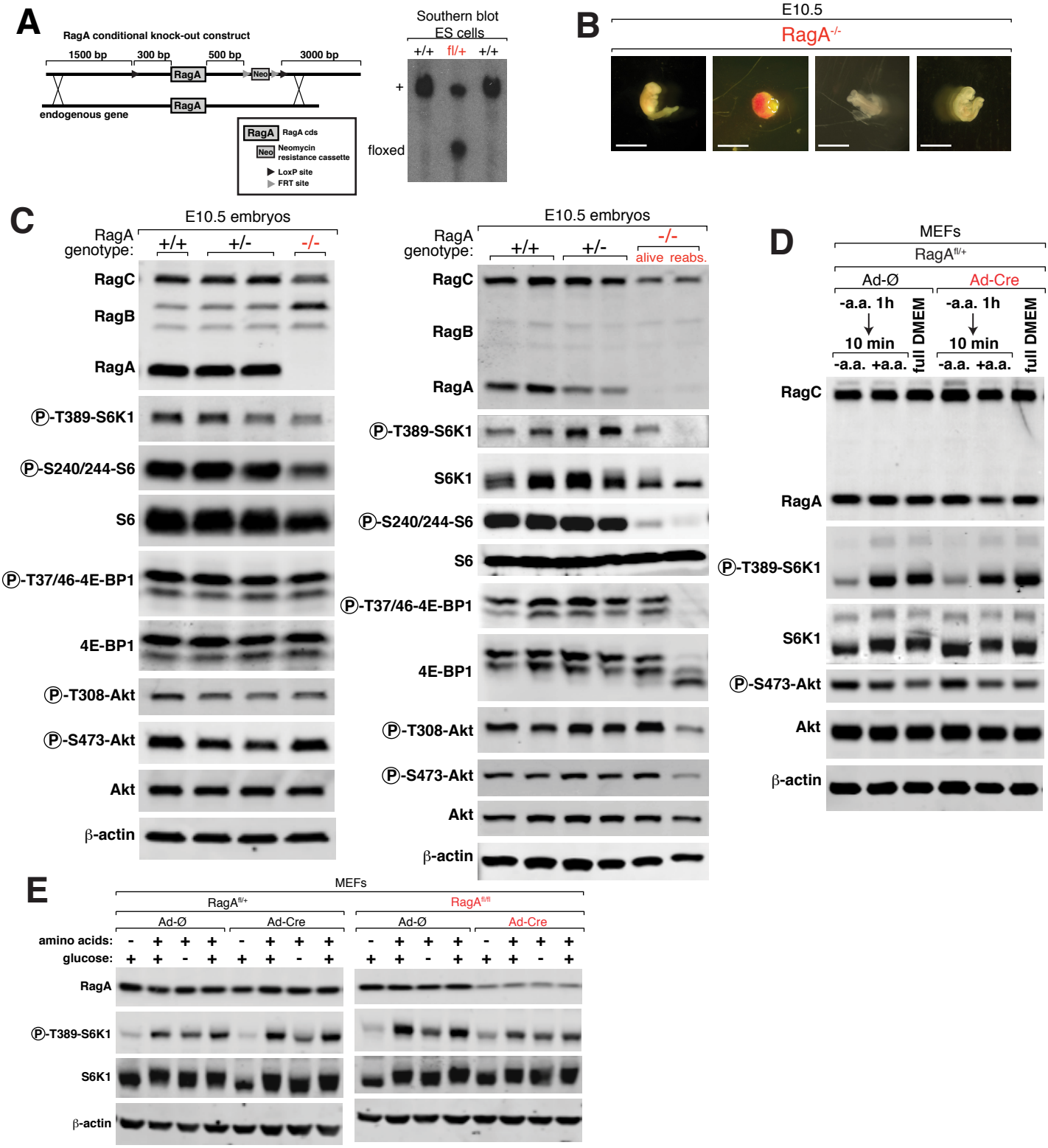

Supplementary Figure 1, relative to Figure 1. (A) Left: Strategy to generate RagA conditional knock-out mice. Right: Southern blot of genomic DNA from targeted ES cells cut with SacI. Fragments correspond to wild-type band 15 Kbp and the RagA floxed allele band 7.5 Kbp. (B) Additional RagA$^{-/-}$ to those on Figure 1a. (C) Whole-embryo protein extracts from RagA$^{+/+}$ RagA$^{+/-}$ and RagA$^{-/-}$ littermates were analyzed by immunoblotting for the indicated proteins (in addition to those in main Figure 1). Note the differential Akt activity in the RagA$^{-/-}$ reabsorbed versus non-reabsorbed embryo in the right panel. (D) Control samples from Figure 1c. RagA$^{fl/+}$ MEFs were infected with controls adenovirus (Ad-Ø) or adenovirus encoding the Cre recombinase (Ad-Cre) and then starved for amino acids for 1 h and, where indicated, re-stimulated for 10 min. Total protein extracts were then analyzed by immunoblotting for the indicated proteins. (E) RagA$^{fl/+}$ and RagA$^{fl/fl}$ MEFs were infected with control adenovirus (Ad-Ø) or adenovirus encoding the Cre recombinase (Ad-Cre) and then starved for amino acids or for glucose for 1 h and, where indicated, re-stimulated for 10 min. Total protein extracts were then analyzed by immunoblotting.

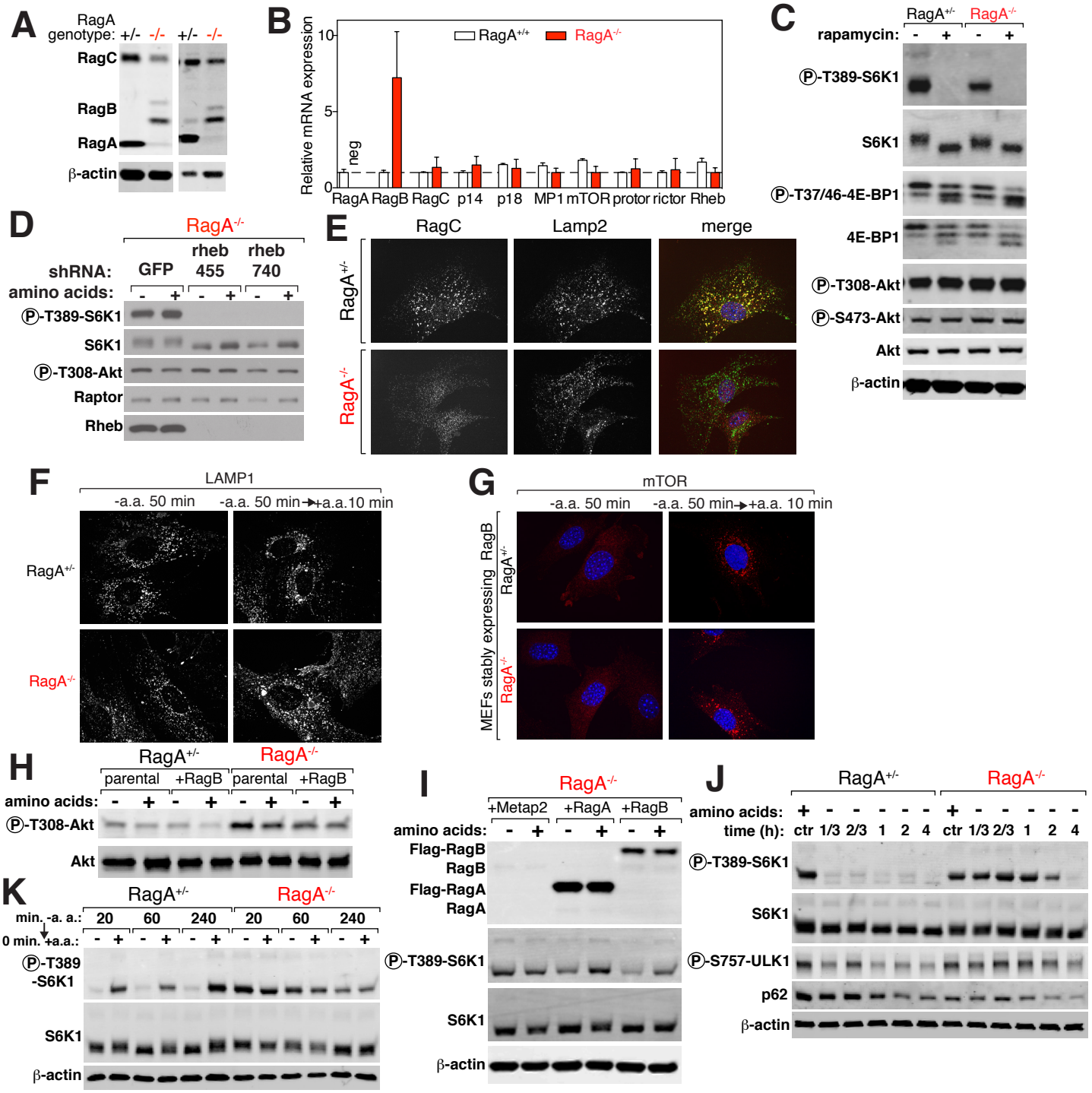

Supplementary Figure 2, relative to Figure 2. (A) Absence of RagA protein and increased RagB protein, determined by immunoblotting, in RagA KO cell lines. (B) mRNA levels of mTORC1-related genes. RagA$^{-/-}$ cells lack RagA mRNA, show increased RagB mRNA, and normal expression of RagC and other mTORC1-related genes. n=3 per genotype; mean±SD (C) RagA$^{-/-}$ cells exhibit sensitivity to mTORC1 inhibition by rapamycin, as determined by immunoblotting for mTORC1 activation markers from whole cell extracts. (D) KD of the Rheb GTPase abrogates mTORC1 activity in RagA-deficient cells. (E) Immunofluorescence for the obligate RagA protein partner RagC and the lysosomal membrane marker Lamp2. (F) Lamp1 localization by immunofluorescence in methanol-fixed cells. RagA$^{+/-}$ and RagA$^{-/-}$ cells show similar pattern of staining, indicating a similar lysosomal morphology. (G) mTOR localization by immunofluorescence in cells stably expressing RagB protein. Expression of RagB in RagA$^{-/-}$ cells allows mTOR to be recruited to the lysosomal surface in the presence of amino acids. (H) Expression of RagB in RagA$^{-/-}$ cells partially suppresses the activation of Akt, as revealed by decreased phosphorylation at Thr308. (I) Expression of RagA or RagB in RagA-null cells leads to amino acid sensitive mTORC1 activity. (J) and (K) Regulation of mTORC1 activity and autophagy by prolonged amino acid starvation of cells. Cells were starved for amino acids for the indicated times and re-stimulated. MTORC1 targets S6K and ULK1, together with the autophagy marker p62 were determined by immunoblotting.

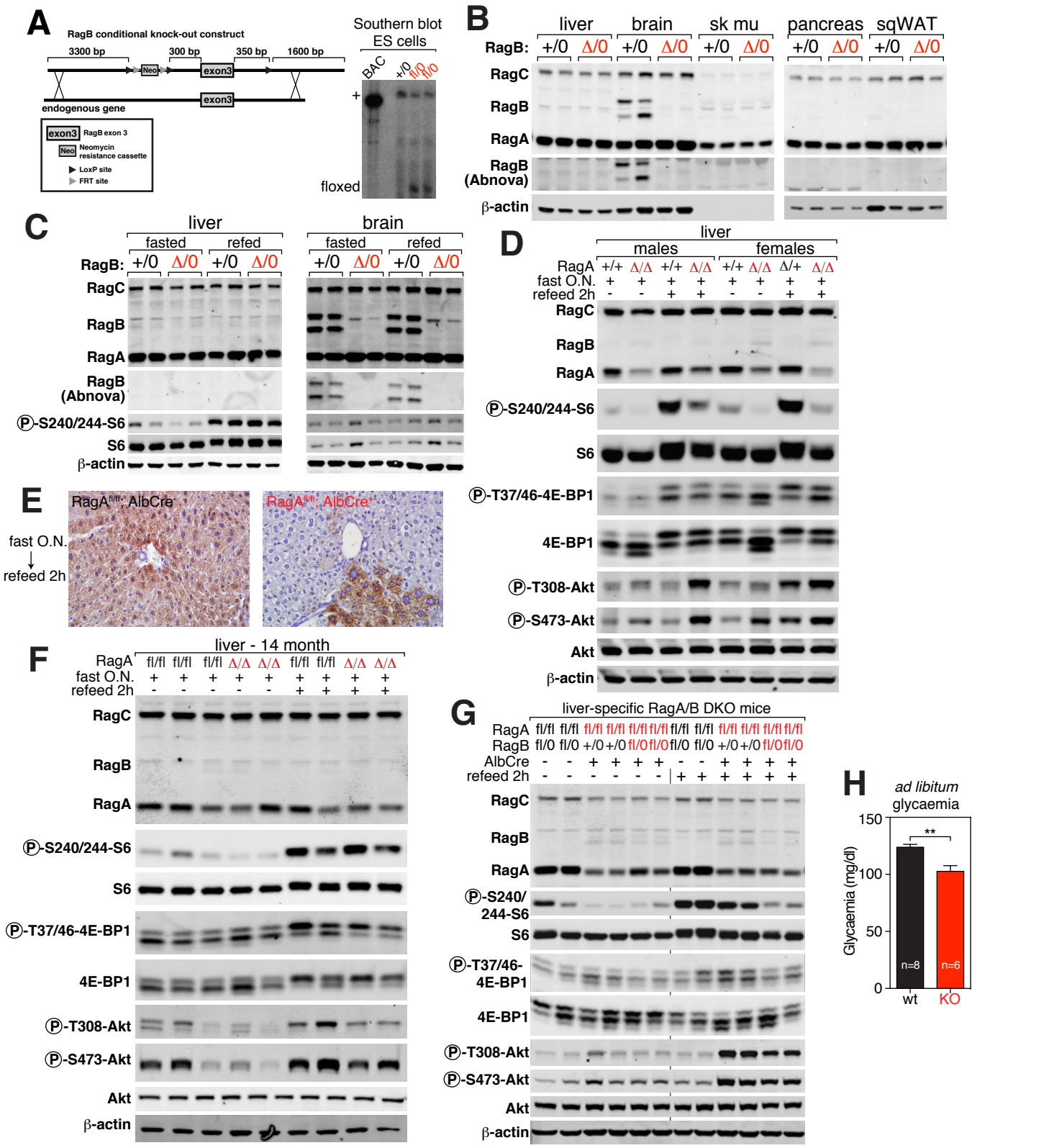

Supplementary Figure 3, relative to Figure 3. (A) Left: Strategy to generate RagB conditional knock-out mice. Right: Southern blot of genomic DNA from targeted ES cells cut with SacI. Fragments correspond to wild-type band (16 Kbp) and the RagB floxed allele band (6 Kbp). (B) Protein extracts of indicated tissues were immunobloted for RagA, B and C. (C) Protein extracts from liver and brain from overnight fasted and refed mice were obtained and mTORC1 activity was determined by immunoblotting. (D) Liver samples from cohorts of young RagA liver-specific KO male and female mice, fasted overnight and re-fed for 2 h, were extracted and levels of the indicated proteins were determined by immunoblotting. (E) Formalin-fixed livers from mice fasted and re-fed as in Figure 3b were processed for immunohistochemistry with anti-phospho-S235/236 S6. The morphology of groups of positive cells in the $RagA^{fl/fl}$; Alb-Cre+ mice is indicative of hepatocytes (F) As in (D), but samples were obtained from older mice (>1 year). (G) Mice with the indicated alleles of RagA & B were fasted and re-fed, as in Figure 3a, and liver protein extracts were immunoblotted for the indicated proteins. (H) Glycaemia was measured from *ad libitum* fed control (WT) and $RagA^{fl/fl}$; Alb-Cre+ (KO) mice.

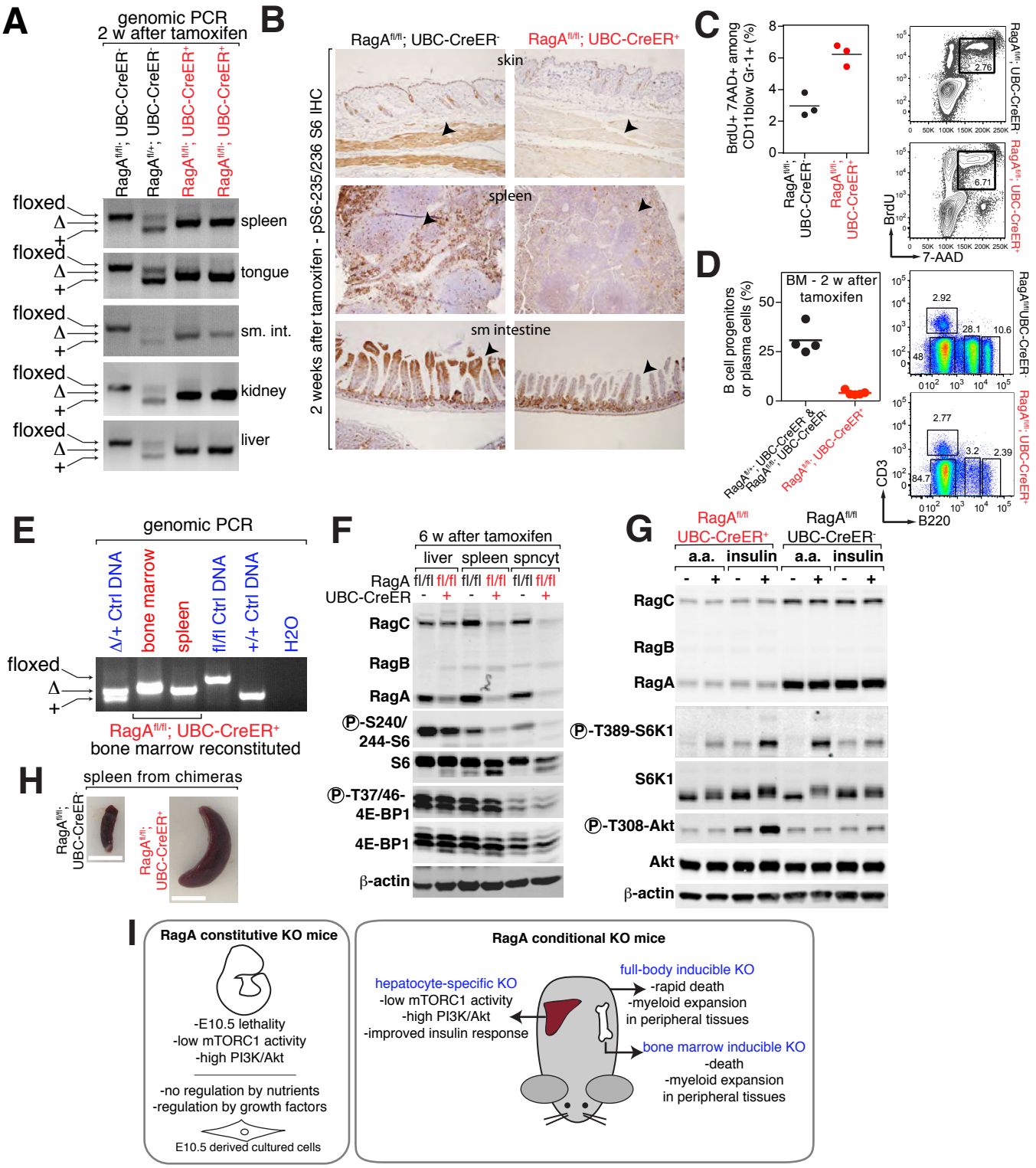

Supplementary Figure 4, relative to Figure 4. (A) Genomic PCR from liver, spleen, kidney, tongue and small intestine (sm. int.) of the indicated genotypes 2 weeks after tamoxifen injections (B) Immunohistochemistry for phospho-S235/236 S6 in samples of the indicated genotypes 2 weeks after the start of tamoxifen injections. (C) Proliferation as determined by *in vivo* BrdU incorporation and 7-AAD staining in bone marrow samples of tamoxifen treated mice of the indicated genotypes on CD11b^{low} Gr-1^{+} CD115^{-} cells, and 2 representative examples of the FACS plots. (D) Bone-marrow derived cells were purified and B cell progenitors and plasma cells were quantified by B220 and CD-3 staining followed by FACS (mean and scatter plot, n=4 and n=5, respectively), and 2 representative examples of the FACS plots. (E) Genomic PCR as in (A), from samples from bone marrow reconstituted mice of the indicated genotypes (F) Whole protein from liver, spleen and purified splenocytes were extracted and immunoblotted for the indicated proteins. (G) Macrophages, after tamoxifen injections, were purified and cultured. Cells were then deprived of serum or amino acids, and re-stimulated with insulin or amino acids, and levels of RagA and mTORC1 activity were determined by immunoblots. (H) Representative spleens from bone marrow-reconstituted mice with RagA$^{fl/fl}$; UBC-CreER- mice and RagA$^{fl/fl}$; UBC-CreER+ cells. (I) Schematic summary of the results presented herein.

Supplementary Table 1. Embryonic lethality of RagA Knock-Out mice, related to Figure 1.

Crosses*	Time	RagA$^{+/+}$	RagA$^{+/-}$	RagA$^{-/-}$
RagA$^{+/-}$ x RagA$^{+/-}$	adult mice	51	121	0
	E13.5	5	6	0
	E11.5	7	13	5 (3^{s}+2^{r})#
	E10.5	26	60	31 (23^{s}+8^{r})

*: Parental mice were either RagA$^{STOP/+}$ or RagA$^{\Delta/+}$; results were similar an added to the present Table.

#: S indicates that the embryo was smaller, but still with identifiable embryonic structures and generally heart beating was detected. R indicates that the embryo was reabsorbed.

Table 2. Embryonic Lethality of RagA/B double Knock-Out mice, related to Figure 3.

Crosses	Time	$RagA^{+/+}$ $RagB^{-/0\ or\ -/-}$	$RagA^{+/-}$ $RagB^{-/0\ or\ -/-}$	$RagA^{-/-}$ $RagB^{-/0\ or\ -/-}$
$RagA^{+/-};RagB^{-/0}$ x $RagA^{+/-};RagB^{-/-}$	E10.5	9	8	3 (0^{s}+3^{r})

#: S indicates that the embryo was smaller, but still with identifiable embryonic structures and generally heart beating were detected. R indicates that the embryo was reabsorbed.

Supplementary Experimental Procedures

Generation of RagA and B knock out mice

All animal studies and procedures were approved by the MIT Institutional Animal Care and Use Committee. RagA locus was targeted by introducing LoxP sites and frt-neomycin-frt cassette flanking RagA exon. Homology arms were 1500 bp and 3000 bp for 5' and 3', respectively. LoxP sites were inserted 300 bp upstream and 500 bp downstream of the RagA exon. The frt-neomycin-frt cassette was inserted next to the 3' LoxP site (map of the targeting allele is shown in Supplementary Figure 1a). Similarly, RagB locus was targeted by introducing LoxP sites flanking exon 3 (map of the RagB targeting allele is shown in Supplementary Figure 3a). $RagA^{STOP}$ allele was previously described (Efeyan et al., 2013). Linearized constructs were electroporated into male v6.5 ES cells of mixed 129Sv/C57B6 background (v6.5). ES colonies were picked and identified by Southern blot and confirmed by PCR amplification of specific insertion products. Positive ES cells clones were then injected into blastocysts and transferred into pseudo-pregnant females to obtain chimeric mice. Pure C57B6 transgenic Cre strains of mice were then bred with RagA or RagB *floxed* mice.

Treatments of mice

Tamoxifen was dissolved in corn oil (Sigma) at 10 mg/ml and 200 μml per 25 g was injected i.p. for 7 consecutive days. For fasting/re-feeding experiments, fasting was performed from 6 pm to 9 am and then mice were injected with 30 % w/v glucose in PBS 100 μl per 30 g mouse, allow to feed *ad libitum*, or injected i.p. with 11.25 μl of insulin (HumulinR, Lilly) dissolved in 5 ml of PBS at a dose of 100 μl per 30 g mouse. For bone marrow reconstitution, host mice were lethally irradiated with 1200 rad divided in two irradiation sessions 4 h apart, and purified $1x10^6$ bone marrow cells from either $RagA^{fl/fl}$; $UBC\text{-}CreER^{+}$ or $RagA^{fl/fl}$; $UBC\text{-}CreER^{-}$ were injected retro-orbitally 1 h after the last irradiation. For glucose tolerance test (GTT), and insulin tolerance test (ITT) mice were fasted overnight (GTT) or 6 h (ITT) and glycaemia was measured for 2 h after i.p. injection of glucose or insulin at the doses described above.

Preparation of MEFs

MEFs from E10.5 embryos were prepared by chemical digestion with trypsin, followed by serial passage when cells reached confluence. MEFs from E13.5 embryos were prepared by chemical digestion with trypsin for 15 min, followed by mechanical disaggregation.

Treatments of MEFs

For amino acids and glucose deprivation in MEFs, sub-confluent cells were rinsed twice and incubated in RPMI without amino acids and/or glucose, and supplemented with 10% dialyzed FBS, as described (Sancak et al., 2008). Stimulation with glucose (5 mM) or amino acids (concentration as in RPMI) was performed for 10 min. For serum withdrawal, cells were rinsed twice in serum-free DMEM and incubated in serum-free DMEM for the indicated times; 100 nM was used for insulin stimulation. Rapamycin was used at 10 nM. For acute deletion of RagA gene in early passage E13.5 MEFs, cells were transduced with adenovirus-encoded Cre, or empty adenovirus as control. For introducing RagB and RagA in RagA E10.5 MEFs, MEFs were infected with the pLJM1 lentivirus encoding for Metap2 (control protein), Flag-RagA or Flag-RagB and selected for stable integration.

Treatments of macrophages

Bone marrow-derived macrophages were isolated as described (Weischenfeldt and Porse, 2008). Briefly, bone marrow from femurs and tibias was plated on 10 cm bacterial grade petri dishes in macrophage media (RPMI containing 10% fetal bovine serum, penicillin and streptomycin, 2 mM glutamine and 30 % v/v L929-conditioned media). Media was replaced two days after isolation. Every two or three days, cells were passaged by scraping with a cell lifter or media was replaced. Five hundred thousand macrophages were seeded in 6-well tissue culture dishes and treated 48 h later. Cells were washed with PBS and incubated for one hour with RPMI lacking amino acids supplemented with dialyzed FBS or DMEM without serum and stimulated with amino acids or 100 nM insulin for 30 minutes.

Immunoblotting

Reagents were obtained from the following sources: anti phospho-T389 S6K1, phospho-S2240/244 S6, phospho-S235/236 S6, phospho-T37/T46 4E-BP1, phosho-T308 Akt,

phospho-S473 Akt, phospho-S9 GSK3-b, phospho-T24/T32 FoxO1/3a, phospho-ERK1/2, phospho-ULK1; total Akt, S6, S6K1, 4E-BP1, GSK3-b, FoxO1, RagA, RagC, ERK1/2, IRS1, p62, from Cell Signaling Technology (CST); anti RagB from Abnova; anti β-actin (clone AC-15) from Sigma. Cells were rinsed once with ice-cold PBS and lysed in ice-cold lysis buffer (50 mM HEPES [pH 7.4], 40 mM NaCl, 2 mM EDTA, 1.5 mM sodium orthovanadate, 50 mM NaF, 10 mM pyrophosphate, 10 mM glycerophosphate, and 1% Triton X-100, and one tablet of EDTA-free complete protease inhibitors [Roche] per 25 ml). Cell lysates were cleared by centrifugation at 13,000 rpm for 10 min. Protein extracts were denatured by the addition of sample buffer, boiled for 5 min, resolved by SDS-PAGE, and analyzed by immunoblotting.

Immunofluorescence and immunohistochemistry

MEFs were plated on fibronectin-coated glass coverslips at a sub-confluent density of 50-100,000 cells/coverslip. The following day, cells were transferred to amino acid-free RPMI, starved for 60 min or starved for 50 min and re-stimulated for 10 min with amino acids, rinsed with cold PBS once and fixed for 15 min with 4% paraformaldehyde, or with -20C methanol for 10 min. PFA-fixed coverslips were permeabilized with 0.05% Triton X-100 in PBS and then all coverslips were incubated with primary antibodies in 5 % normal donkey serum for 1 h, rinsed, and incubated with Alexa fluor-conjugated secondary antibodies (Invitrogen) diluted 1:400, for 45 min. Coverslips were mounted on glass slides using Vectashield (Vector Laboratories) and imaged on a spinning disk confocal system (Perkin Elmer) equipped with 405 nm, 488 nm and 561 nm laser lines, through a 63X objective.

Flow Cytometry

Total bone marrow and spleen cells were stained with the following conjugated monoclonal antibodies: CD3, CD19, B220, NK1.1, Ter119, CD11c, CD11b, Gr-1 (Ebioscience). Stained cells were analyzed on a LSR cytometer (BD Biosciences) and data analyzed on FloJo software (TreeStar). For BrdU incorporation, 1.5mg of BrdU was injected intraperitoneally into mice previously treated with tamoxifen 10-12 days before. After 6h, mice were sacrificed and BrdU incorporation was analyzed by flow cytometry by standard nuclear staining following manufacturer's instruction (BD Pharmingen).

Quantitative PCR

Total RNA was extracted with RNAeasy (Qiagen), retro-transcribed with Superscript III (Invitrogen) and used at 1:100 dilution in quantitative real time PCR in an Applied Biosystems thermocycler. 36B4 and β-actin were for normalization. The following primers were used:

RagA F	GAACCTGGTGCTGAACCTGT
RagA R	GATGGCTTCCAGACACGATT
RagB F	TTCGATTTCTGGGAAACCTG
RagB R	AGTTCACGGCTCTCCACATC
mTOR F	GGTGCTGACCGAAATGAGGG
mTOR R	TCTTGCCCTTGTGTTCTGCA
Raptor F	TGGCAGCCAAGGGCTCGGTA
Raptor R	GCAGCAGCTCGTGTGCCTCA
Pepck F	CGATGACATCGCCTGGATGA
Pepck R	TCTTGCCCTTGTGTTCTGCA
G-6-P F	GAAGGCCAAGAGATGGTGTGA
G-6-P R	TGCAGCTCTTGCGGTACATG
Glucokinase F	GAGATGGATGTGGTGGCAAT
Glucokinase R	ACCAGCTCCACATTCTGCAT
36B4 F	TAAAGACTGGAGACAAGGTG
36B4 R	GTGTACTCAGTCTCCACAGA
Actin F	GGCACCACACCTTCTACAATG
Actin R	GTGGTGGTGAAGCTGTAGCC

Statistical analyses

For Kaplan-Meier survival curves, comparisons were made with the Log-rank Mantel-Cox method. For qtPCR analyses, measurements of glycemia, and other comparison between pairs, non-parametric t-tests were performed.